Article

Cell Reports

# Dopamine Gates Visual Signals in Monkey Prefrontal Cortex Neurons

## Graphical Abstract

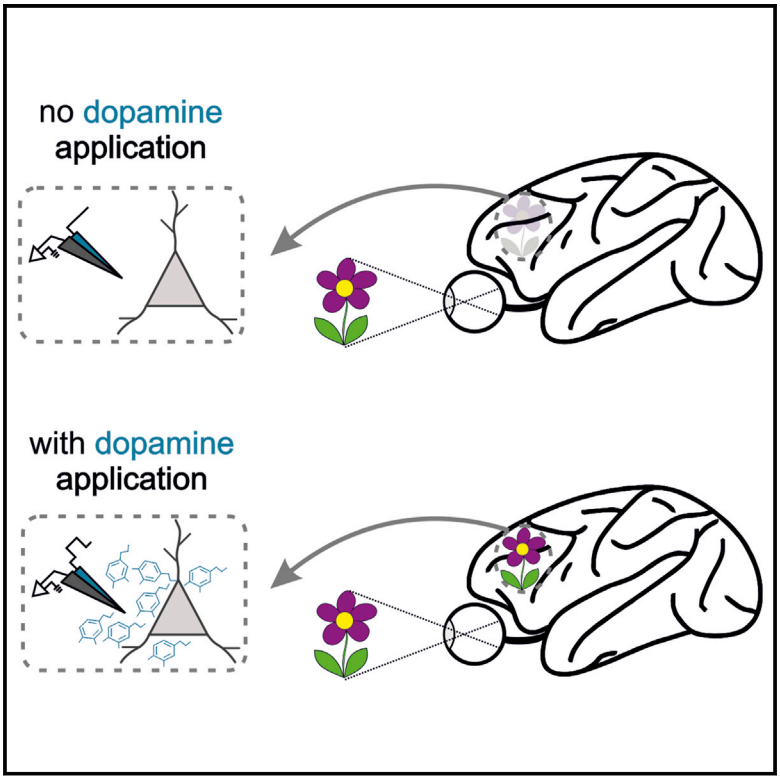


## Authors

Maximilian Stalter, Stephanie Westendorff, Andreas Nieder

## Correspondence

andreas.nieder@uni-tuebingen.de

## In Brief

Stalter et al. show that pharmacological stimulation of specific dopamine receptors enhances the single-neuron and population coding quality in prefrontal cortex neurons. The results elucidate the mechanisms of how receptor-specific dopamine effects can act as a gating signal that enables privileged access of sensory information to PFC circuits.

## Highlights

- Stimulation of dopamine receptors enhances sensory sensitivity of PFC neurons
- Stimulation of D1Rs and D2Rs increases signal-to-noise ratio
- Neither D1R nor D2R stimulation affects the neurons' tuning sharpness
- Dopamine provides a gating signal to enable access of sensory information to PFC

Stalter et al., 2020, Cell Reports *30*, 164–172
January 7, 2020 
https://doi.org/10.1016/j.celrep.2019.11.082

CellPress

OPEN ACCESS
CellPress

Cell Reports
Article

# Dopamine Gates Visual Signals in Monkey Prefrontal Cortex Neurons

Maximilian Stalter,[1] Stephanie Westendorff,[1] and Andreas Nieder[1,2,*]
[1]Animal Physiology, Institute of Neurobiology, Eberhard-Karls-Universität Tübingen, Auf der Morgenstelle 28, 72076 Tübingen, Germany
[2]Lead Contact
*Correspondence: andreas.nieder@uni-tuebingen.de
https://doi.org/10.1016/j.celrep.2019.11.082

## SUMMARY

**The neurotransmitter dopamine, which acts via the D1-like receptor (D1R) and D2-like receptor (D2R) family, may play an important role in gating sensory information to the prefrontal cortex (PFC). We tested this hypothesis in awake macaques and recorded visual motion-direction tuning functions of single PFC neurons. Using micro-iontophoretic drug application combined with single-unit recordings, we simulated receptor-specific dopaminergic input to the PFC and explored cellular gating mechanisms. We find that stimulating D1Rs, and particularly D2Rs, enhances the single-neuron and population coding quality in PFC neurons. D2R stimulation causes a clear increase of the neurons' responses to the preferred motion direction and a decrease to the non-preferred motion direction, thus enhancing neuronal signal-to-noise ratio. Neither D1R nor D2R stimulation had any impact on the neurons' tuning sharpness. These results elucidate the mechanisms of how receptor-specific dopamine effects can act as a gating signal that enables privileged access of sensory information to PFC circuits.**

## INTRODUCTION

The primate prefrontal cortex (PFC) is considered to act as the brain's central executive (Miller and Cohen, 2001). It is engaged in various cognitive control processes, such as categorization (Freedman et al., 2001; Nieder et al., 2002), working memory (Funahashi et al., 1989; Jacob and Nieder, 2014; Rainer et al., 1998a), rule switching (Eiselt and Nieder, 2013; Vallentin et al., 2012; Wallis et al., 2001), and decision making (Kim and Shadlen, 1999; Merten and Nieder, 2012). However, the first component of successful cognitive control is representing sensory stimuli from the environment (Ott and Nieder, 2019). As a reflection of this requirement, PFC neurons also represent basic sensory signals and are tuned, for instance, to luminance, visual motion direction, and speed of visual stimuli (Constantinidis et al., 2001; Hussar and Pasternak, 2009, 2013; Zaksas and Pasternak, 2006). In contrast to neurons in early sensory areas that encode information of the physical stimulus attributes, PFC neurons filter, or gate, relevant sensory information (Asaad et al., 2000; Everling et al., 2002; Rainer et al., 1998b), albeit by unknown mechanisms.

The neuromodulator dopamine has been suggested to play a prominent part in this sensory gating process (Ott and Nieder, 2019). Dopamine is synthesized and released by dedicated neurons in the midbrain that send their axons to many brain regions, including the PFC (Björklund and Dunnett, 2007; Williams and Goldman-Rakic, 1998). Dopamine as a neuromodulator enhances or suppresses cellular activity indirectly by influencing synaptic information transmission. Dopamine binds to five different dopamine receptors that fall into two main receptor types (Seamans and Yang, 2004), the D1-like receptor (D1R) family, with subtypes $D_1$ and $D_5$, and the D2R, with subtypes $D_2$, $D_3$, and $D_4$.

Salient, behaviorally relevant stimuli activate dopamine neurons that quickly release dopamine, and dopamine neurons are known to signal a reward prediction error that enables reinforcement learning (Eshel et al., 2015; Schultz, 2016; Schultz et al., 1997; Stauffer et al., 2016; Steinberg et al., 2013). However, this dopamine signal is also ideally suited to prompt the PFC for the processing of incoming sensory signals (de Lafuente and Romo, 2011, 2012; Redgrave and Gurney, 2006). It is therefore hypothesized that dopamine transients in PFC provide a "gating signal" which determines when and to what extent the PFC accepts new input to become updated and stored in working memory (Braver and Cohen, 1999; Cohen et al., 2002; Ott and Nieder, 2019). Within this framework, dopamine may influence how well incoming sensory information is encoded by PFC neurons, with only relevant sensory information accessing later PFC processing stages. As hypothetical gating mechanisms, an enhancement of the neurons' signal-to-noise ratio by D1R-mediated inhibitory mechanisms, complemented by a gain computation enhancing coding via D2R-mediated excitatory mechanisms, was proposed (Ott and Nieder, 2019).

Here, we tested these hypotheses in the PFC of rhesus macaques. Instead of using a restricted set of stimuli, which previously prevented a detailed characterization of its neuronal gating mechanisms (Jacob et al., 2013), we studied the receptor type-specific effects of dopamine on sensory signals by recording detailed visual tuning functions of single neurons to dot patterns moving in different directions. In order to simulate dopaminergic input to the PFC, we used micro-iontophoretic drug application in combination with single-unit recordings. Effects of D1R stimulation (using SKF81297) and D2R stimulation (by applying quinpirole) on visual tuning characteristics

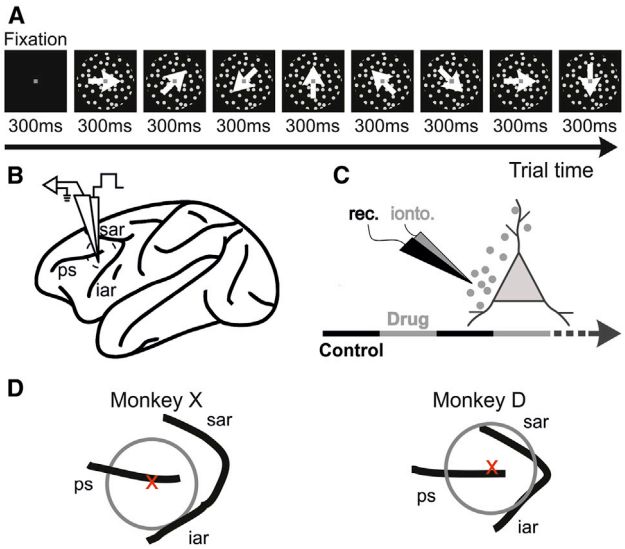


**Figure 1. Task Protocol and Drug Application Regime**

(A) Passive viewing task. Stimuli were random dot patterns moving in one of eight directions. The monkeys initiated a trial by holding a metal bar and fixating on a central spot on the screen. A succession of stimuli was presented, each containing a different direction of motion. The monkeys maintained fixation throughout the whole stimulus presentation.

(B) Schematic of a rhesus monkey brain. The location of simultaneous single-unit recording and iontophoretic drug application within the PFC is shown. For recording a combination of a recording electrode and a glass micropipette was used. IAR, inferior sulcus arcuatus; PS, principal sulcus; SAR, superior sulcus arcuatus.

(C) Drug application regime. During recording, blocks without drug application alternated with blocks of drug application. Charged DA molecules are micro-iontophoretically applied to the extracellular vicinity of the neurons.

(D) Anatomical surface reconstruction of the recording site for monkey X (left) and monkey D (right). Recordings were performed dorsal and ventral to the posterior end of the principal sulcus (PS). The red X indicates the center of the recording chamber. IAR, inferior sulcus arcuatus; SAR, superior sulcus arcuatus.

were compared with control conditions without pharmacological intervention.

## RESULTS

To investigate the influence of dopamine on visual motion tuning of single neurons in the PFC, we trained two macaque monkeys to passively view moving random dot patterns that moved in eight different directions (Figure 1A). Both animals were experienced with discriminating motion stimuli. On average, monkey X completed 35 sessions, and monkey D completed 48 sessions. While the monkeys maintained fixation, we recorded in the principal sulcus region (Figure 1B) of the dorsolateral PFC. Through micro-iontophoretic application of dopaminergic agents during recordings, we were able to explore the influence of the dopamine system on direction-selective neurons. We compared the neurons' responses during a control condition (blocks of trials with no drug application) with blocks of trials in which either a D1R agonist (SKF81297) or a D2R agonist (quinpirole) was administered (Figure 1C).

### Dopamine Receptor Family Agonists Modulate Neurons' Responses to Preferred and Least Preferred Motion Directions

We recorded single-unit activity of 296 units (n = 81 and n = 215 for monkeys X and D, respectively) around the principal sulcus of the PFC (Figure 1D) while monkeys watched moving random dot stimuli. To quantify the direction selectivity of the recorded single-units, we performed a two-factor ANOVA with factors direction of motion and iontophoresis condition on the discharge rates during stimulus presentation. All neurons with significant effects of the main factor, direction of motion ($p < 0.05$), were counted as direction selective. This analysis revealed a substantial fraction of 28% (n = 82) of randomly recorded neurons that encoded visual motion direction. We did not observe a difference in the frequency of direction-selective neurons between the two monkeys, $\chi^2(1, 296) = 1.439$, $p = 0.23$.

Figure 2 shows the responses of two direction-selective neurons. The first neuron, which was tested with the D1R agonist SKF81297, was tuned to a left upward motion direction. The second neuron, which was probed with the D2R agonist quinpirole was, tuned to a right upward motion. Detailed responses of the first neuron in the control (Figure 2A) and drug (Figure 2B) conditions are depicted as time-resolved dot-raster and spike-density histograms. This neuron's discharge rates per motion direction are displayed as a polar plot (Figure 2C) and tuning curve fitted by a Gaussian function (Figure 2D). The responses of the second neuron are displayed in the same layout in the right column (Figures 2E–2H). Across the population of direction-selective neurons, direction selectivity was uniformly distributed ($p = 0.28$, n = 82, Rayleigh test for circular uniformity).

Application of the D1R agonist SKF81297 to the neuron in the left column systematically increased the discharge rates (corrected by baseline) compared with the control condition (Figures 2C and 2D). The discharge rates to the preferred direction tended to increase with application of the D1R agonist (mean control = +8.56 ± 1.2 Hz [SEM], n = 28; mean drug = +10.78 ± 1.58 Hz [SEM], n = 20; $p = 0.06$, Wilcoxon rank-sum test). For the same neuron, responses to the least preferred direction mildly increased with D1R stimulation (mean control = −0.01 ± 0.63 Hz [SEM], n = 28; mean drug = +0.61 ± 0.97 Hz [SEM], n = 20; $p < 0.001$, Wilcoxon rank-sum test). The difference in the discharge rates between the preferred direction and the least preferred direction increased. Consequently, the neuron shows enhanced direction sensitivity under D1R stimulation because it discriminated better between the preferred and least preferred direction.

In the second neuron (Figures 2G and 2H), which was stimulated with the D2R agonist, the responses to the preferred direction non-significantly increased during the drug condition (mean control = +4.38 ± 1.56 Hz [SEM], n = 25; mean drug = +8.49 ± 2.65 Hz [SEM], n = 20; $p = 0.62$, Wilcoxon rank-sum test). At the same time, the discharge rates to the least preferred direction were significantly reduced with D2R stimulation (mean control = −0.15 ± 0 Hz [SEM], n = 28; mean drug = −0.35 ± 0 Hz [SEM], n = 20; $p < 0.0001$, Wilcoxon rank-sum test). Therefore, D2R stimulation with quinpirole also enhanced the direction sensitivity in this neuron.

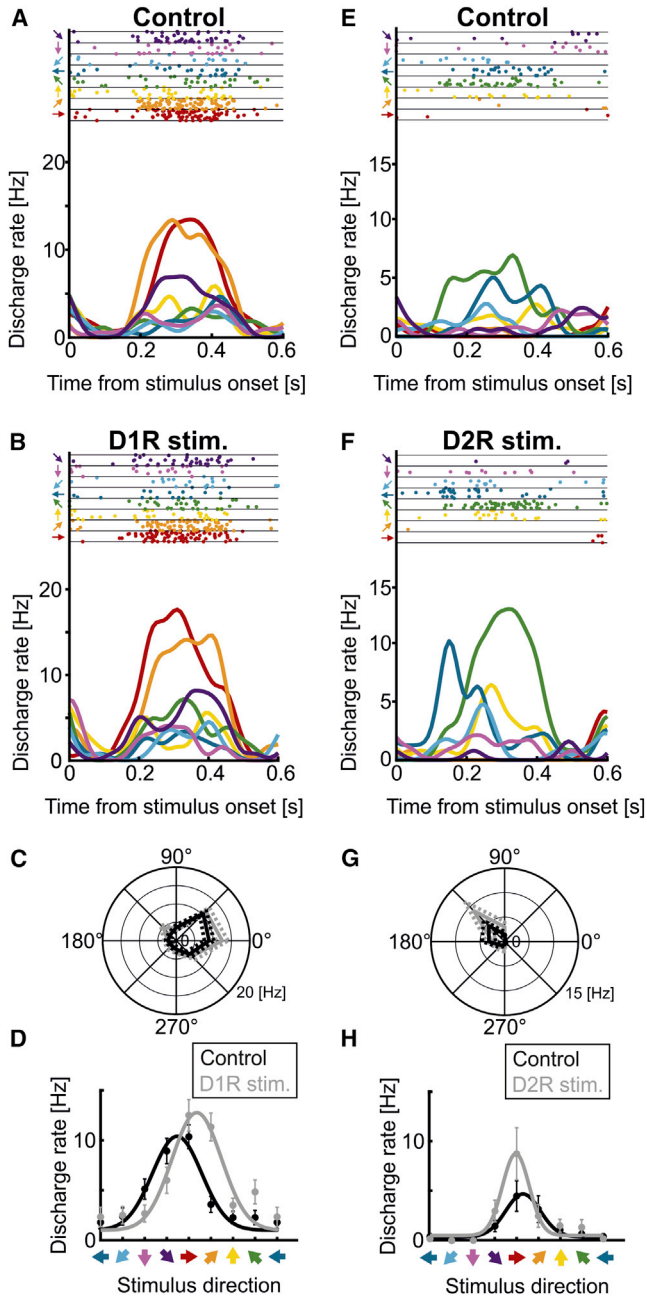


**Figure 2. Visual Motion Direction Selectivity of Two PFC Neurons in Control and Drug Conditions**

(A and E) Discharge profile of two neurons during stimulus presentation when no drug was applied (control condition). The top shows dot-raster plots for the eight directions of motion (each line is a trial, each dot represents one action potential). Colored arrows left of the dot raster indicate the direction the random dots moved in. The bottom shows the corresponding spike-density function (discharge rate smoothed with a Gaussian kernel with an SD of 25 ms).

(B and F) Same conventions as for (A) and (E) but during the micro-iontophoretic application of the D1R agonist SKF81297 (drug condition) or the D2R agonist quinpirole.

(C, D, G, and H) Neuronal tuning profile as a polar plot (C and G) and fitted with a Gaussian model (D and H), during the control condition (black lines) and during application of the dopamine receptor agonists (gray lines). Error bars represent SEM across trials.

N is the number of trials per direction of motion: for (A), n = 28; for (B), n = 20; and for (C) and (D), n = 28 and n = 20 for control or drug conditions, respectively. For (E), n = 25; for (F), n = 20; for (G) and (H), n = 25 and n = 20 for control or drug conditions, respectively.

Overall, a substantial fraction of direction-selective neurons was affected by the stimulation with the D1R and D2R agonists. Stimulation of the D1 receptor significantly changed the discharge rates to the preferred direction in 27% of the neurons (10 of 37; 8 neurons increased and 2 neurons decreased discharge rates, respectively). Responses to the least preferred direction were significantly modulated in 65% (24 of 37; 15 neurons increased and 9 neurons decreased discharge rates, respectively) of the neurons recorded with the D1R agonist. For the population of neurons that were stimulated with the D2R agonist, 24% (11 of 45; increases and decreases in discharge rate in 7 and 4, respectively) significantly changed their responses to the preferred direction, and 69% of the neurons showed significantly modulated responses to the least preferred direction with D2R stimulation (31 of 45; increases and decreases in discharge rate in 26 and 5, respectively).

The example neurons in Figure 2 suggest that stimulation of the dopamine receptors differentially affects the neurons' responses to different motion directions. We therefore explored to what extent D1R and D2R stimulation changed the baseline-corrected discharge rates to the preferred (eliciting maximum firing) and/or the least preferred direction (eliciting minimum firing) across the population of individual direction-selective neurons. This was done for all neurons recorded with the D1R agonist SKF81297 and the D2R agonist quinpirole, the average tuning functions of which are plotted in Figures 3A and 3B, respectively. In order to assess the influence of the drugs on the preferred direction, we calculated the difference of responses to the preferred direction during receptor stimulation and control (drug − control). Stimulation of D1R had no impact on the preferred direction (Figure 3C) (Δ preferred direction = +0.24 ± 0.33 Hz [SEM], n = 37; p = 0.31, paired Wilcoxon test). The analogous calculations were done with discharge rates to the least preferred direction. D1R stimulation had no significant impact on responses to the least preferred direction (Figure 3C) (Δ least preferred direction = −0.34 Hz ± 0.25 Hz [SEM], n = 37; p = 0.29, paired Wilcoxon test). When we directly compared the responses differences (D1R stimulation − control) to the preferred and least preferred direction, the values also did not differ within neurons (p = 0.10, paired Wilcoxon test).

In contrast, D2R stimulation showed a strong impact on responses to both the preferred and least preferred directions. Stimulation of D2R led to a strong increase in responses to the preferred direction (Figure 3D) (Δ preferred direction = +2.2 ± 0.48 Hz [SEM], n = 45; p < 0.0001, paired Wilcoxon test). In addition, stimulation of the D2R led to a significant decrease in responses to the least preferred direction (Figure 3D) (Δ least preferred direction = −0.71 ± 0.34 Hz [SEM], n = 45; p = 0.008, paired Wilcoxon test). Thus, while D2R stimulation clearly enhanced tuning selectivity by increasing responses to the preferred direction, while at the same time reducing the

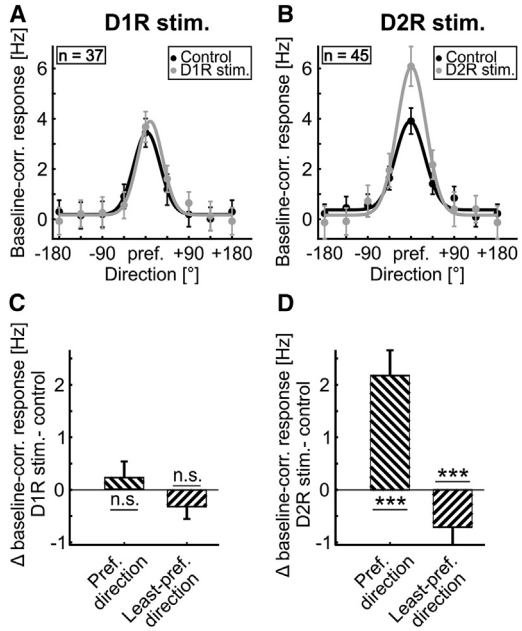


**Figure 3. Gaussian Tuning Curves and Modulation of Responses to the Preferred and Least Preferred Direction**

(A) Population tuning curves with Gaussian fit during control (black line) and with stimulation of the D1R agonist SKF81297 (gray line; n = 37).

(B) Same conventions as in (A) but for the application of the D2R agonist quinpirole (n = 45).

(C) Modulation of the preferred and least preferred direction under D1R stimulation. Stimulation of D1Rs with SKF81297 has no effect on either preferred or least preferred motion direction (n = 37).

(D) Same conventions as in (C) but for stimulation of the D2R (n = 45). Stimulation of D2Rs with quinpirole increases the responses to the preferred direction, while decreasing the responses to the least preferred direction.

***$p < 0.0001$; n.s., $p > 0.05$; error bars represent SEM across neurons given by n.

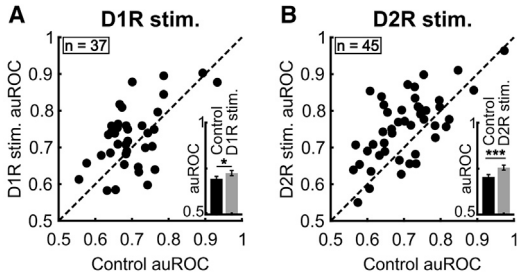


**Figure 4. Modulation of Direction Sensitivity after Dopamine Receptor Stimulation**

(A and B) Comparison of tuning sensitivity (as measured by auROC values) during the control and drug conditions of the populations of direction-selective neurons recorded with the D1R agonist SKF81297 (n = 37) or the D2R agonist quinpirole (n = 45), respectively.

(A) Each dot represents the auROC values for an individual neuron recorded with SKF81297. Inset: mean auROC values across all neurons for the control and drug conditions. The directional sensitivity of neurons significantly increased during stimulation of D1Rs with SKF81297.

(B) Same conventions as in (A) with application of D2R agonist quinpirole. The directional selectivity of neurons was significantly increased during the stimulation of D2Rs with quinpirole. *$p < 0.05$ and ***$p < 0.0001$; error bars represent SEM across neurons given by n.

responses to least preferred direction, this effect was much more subtle for D1R.

## Dopamine Receptor Stimulation Enhances Neuronal Direction Sensitivity

After the positive effects of D1R and D2R-stimulation were verified at the level of discharges to the preferred and least preferred motion directions, we determined the effects on the neurons' overall response sensitivity. As a measure of neuronal sensitivity, we calculated the area under the receiver-operating characteristic curve (auROC) between the preferred and least preferred directions in the control and drug conditions separately (Figure 4). This was done for all direction-selective neurons recorded during D1R stimulation with SKF81297 (37 of 82; Figure 4A) and D2R stimulation with quinpirole (45 of 82; Figure 4B). Here, an auROC value of 0.5 would indicate that the preferred and least preferred motion directions elicit equal discharge rates, whereas values higher than 0.5 up to 1 signify consistently higher discharge rates to the preferred direction. To compare auROC values between drug and control conditions, we plotted the values per neuron against each other. If the tuning sensitivity remained equal for the drug and control conditions, the data points would be expected to lie on the unity line, on average. In contrast, higher tuning sensitivity in the drug condition would result in more data points lying above the unity line. Indeed, we found that sensitivity of the population of neurons was shifted upward in both drug conditions, indicating enhanced sensitivity for both D1R and D2R stimulation (Figures 4A and 4B).

Direction sensitivity significantly increased with stimulation of the D1R (Figure 4A; Δ auROC = +0.03 ± 0.013 [SEM], n = 37; $p < 0.05$, paired Wilcoxon test). Similarly, direction sensitivity also, but to a higher degree, increased with stimulation of the D2R (Figure 4B; Δ auROC = +0.051 ± 0.011 [SEM], n = 45; $p < 0.0001$, paired Wilcoxon test). This shows that the sensitivity to basic sensory stimuli in the PFC is enhanced through stimulation with a D1R agonist as well as a D2R agonist.

## Discharge Variability Is Unaffected by Dopamine Receptor Stimulation

The positive effects of D1R and D2R stimulation on response sensitivity (auROC analysis) can, in addition to changes in the mean discharge rates to preferred and/or non-preferred directions, also result from a modulation of the neuronal response variability. To test whether dopamine receptor stimulation changed neuronal response variability, and thereby enhanced tuning sensitivity, we next calculated the trial-by-trial discharge variability using the Fano factor (FF) (Cohen and Maunsell, 2009). The FF is also known as the mean-normalized dispersion and constitutes the ratio "variance/mean." We calculated the FF in the control and drug conditions separately for neurons recorded with application of SKF81297 and quinpirole. This was done for the responses to the preferred and least preferred directions.

Neuronal variability was not changed during D1R stimulation. The application of the D1R agonist did not reduce the FF for responses to the preferred direction (Δ FF = −0.98 ± 0.54 [SEM], n = 37; p = 0.08, paired Wilcoxon test). It also did not change

the FF for responses to the least preferred direction (Δ FF = −0.16 ± 0.46 [SEM], n = 37; p = 0.69, paired Wilcoxon test).

D2R stimulation did also not reduce the FF to the preferred direction compared with the control condition (Δ FF = −0.25 ± 0.68 [SEM], n = 45; p = 0.19, paired Wilcoxon test). Similarly, the FF of responses to the least preferred direction was unchanged by D2R stimulation (Δ FF = −0.17 ± 0.45 [SEM], n = 45; p = 0.26, paired Wilcoxon test). Therefore, stimulation with neither the D1R nor D2R agonist significantly altered the trial-by-trial variability of neurons tuned to visual motion direction signals. However, a trend was observed that D1R stimulation reduced response variability to the preferred direction.

## Stimulation of Dopamine Receptors Does Not Change Tuning Width

So far we have shown that dopamine agonists enhance neurons' sensitivity (i.e., the coding quality, or signal-to-noise ratio) by increasing and/or decreasing responses to preferred and non-preferred stimuli, respectively. However, an alternative, or additional, way to enhance specificity of sensory input would be to increase the neurons' tuning selectivity by sharpening the tuning curve and thereby confining responses to more specific directions.

To explore potential changes of tuning selectivity with dopamine receptor stimulation, we quantified the neuronal tuning curves by fitting a Gaussian function to the responses of each selective neuron during the control and drug conditions separately. We first evaluated how well the Gaussian model fit the real data by deriving the goodness of fit ($R^2$) for each neuron. The quality of the fits was suitable and not different between control and drug trials, neither for the D1R agonist (mean $R^2$: control, 0.6 ± 0.048 [SEM]; drug, 0.6 ± 0.039 [SEM]; n = 37; p = 0.82, paired Wilcoxon test) nor for the D2R agonist (mean $R^2$: control, 0.65 ± 0.039 [SEM]; drug, 0.64 ± 0.039 [SEM]; n = 45; p = 0.55, paired Wilcoxon test).

When comparing the tuning width of the neurons in the drug and control conditions, we found that the application of the D1R agonist renders the tuning width of the Gaussian unchanged (mean width: control, 106.8° ± 17.2° [SEM]; drug, 96.2° ± 15.1° [SEM]; n = 37; p = 0.13, paired Wilcoxon test). The same was true for the D2R agonist (mean width: control, 84.1° ± 13.7° [SEM]; drug, 96.6° ± 14.7° [SEM]; n = 45; p = 0.42, paired Wilcoxon test) . For a graphical depiction of the population tuning curves, we averaged over all neurons in control and drug trials for both the D2R and D1R agonists independently (Figures 3A and 3B). Although the amplitudes of the fits varied to different extents for D1R and D2R, the widths of the Gaussian fits in control and drug conditions stayed constant.

As a second measure of tuning width, we calculated the full width at half height of the unfitted tuning functions and compared these values between control and drug trials for the two dopamine receptor agonists. This analysis confirmed the results obtained from the Gaussian fits in that application of neither the D1R agonist (mean tuning width: control, 104.3° ± 13° [SEM]; drug, 105.8° ± 11.1° [SEM]; n = 37; p = 0.88, paired Wilcoxon test) nor the D2R agonist (mean tuning width: control, 111° ± 9.7° [SEM]; drug, 103.2° ± 8.4° [SEM]; n = 45; p = 0.61, paired Wilcoxon test) altered the tuning width. Thus, both measures of tuning selectivity argue that input gating is not achieved by sharper tuning to motion direction.

## Dopamine Receptor Stimulation Enhances Population Decoding of Directions

The effects of the dopamine receptor agonists on the tuning behavior of single neurons suggest that the neurons' individual tuning quality was enhanced both after D1R and D2R stimulation as a way to gate motion direction information. To find out whether, during dopamine stimulation, the population of tuned neurons would indeed provide higher quality information about the sensory input (i.e., the entire range of motion directions), we applied a population decoding analysis. To that aim, we trained multi-class support vector machine (SVM) classifiers to discriminate motion directions on the basis of the spiking activity of tuned neurons during stimulus presentation.

First, the classifiers were trained with activity when no drug was applied (control) and separately for the two populations of neurons that were later stimulated with either the D1R (n = 37) or the D2R (n = 45) agonist. After training, the classifiers were tested with novel data from the same two neuronal populations to explore how well it could predict directions on the basis of the information extracted from trials used for classifier training. The resulting confusion matrices illustrate the classifiers' robust decoding performances for both neuron populations (that were later tested with drugs) in the control condition (Figures 5A and 5B). On average, performance accuracy was 37.8% ± 2.6% (SEM) for the population later tested with the D1R agonist (Figure 5A) and 40.5% ± 2.6% (SEM) for the population later tested with the D2R agonist (Figure 5B). Overall, decoding performance was well above chance (12.5% for eight directions) for both neuron populations (p < 0.0001, random permutation test).

Next, we compared decoding performance between control and dopamine receptor stimulation conditions. We trained and tested new classifiers on the spiking activity of the same two neuronal populations, but this time during D1R or D2R stimulation. Compared with decoding during the control, D1R stimulation mildly but significantly increased decoding performance by 8% (Figure 5C; mean accuracy: 46% ± 2.9% [SEM]; p < 0.05, randomization test). D2R stimulation resulted in even higher decoding performance and enhanced accuracy by 14% (Figure 5D; mean accuracy: 54.1% ± 3.2% [SEM]; n = 45; p = 0.005, randomization test). This improvement is also visible in the overall tuning curve constructed from the classifiers' performances (Figures 5E and 5F).

This improvement with dopamine receptor stimulation was not confined to few very motion direction-selective cells. In fact, decoding performance showed similar improvements when the 10% most selective neurons (i.e., those with the smallest individual p values for motion selectivity) were excluded from the classifier analysis. For D1R stimulation, classification improved by 7.8% (from 31.9% in the control condition to 39.7% under D1R stimulation, p = 0.064), which was comparable with the enhancement of 8.0% for the entire neuron population (see values above). Similarly, D2R stimulation enhanced classification by 13.6% (from 34.3% in the control condition to 47.9% under D1R stimulation, p = 0.001), which was identical to the enhancement of 13.6% for the entire neuron population. This argues that

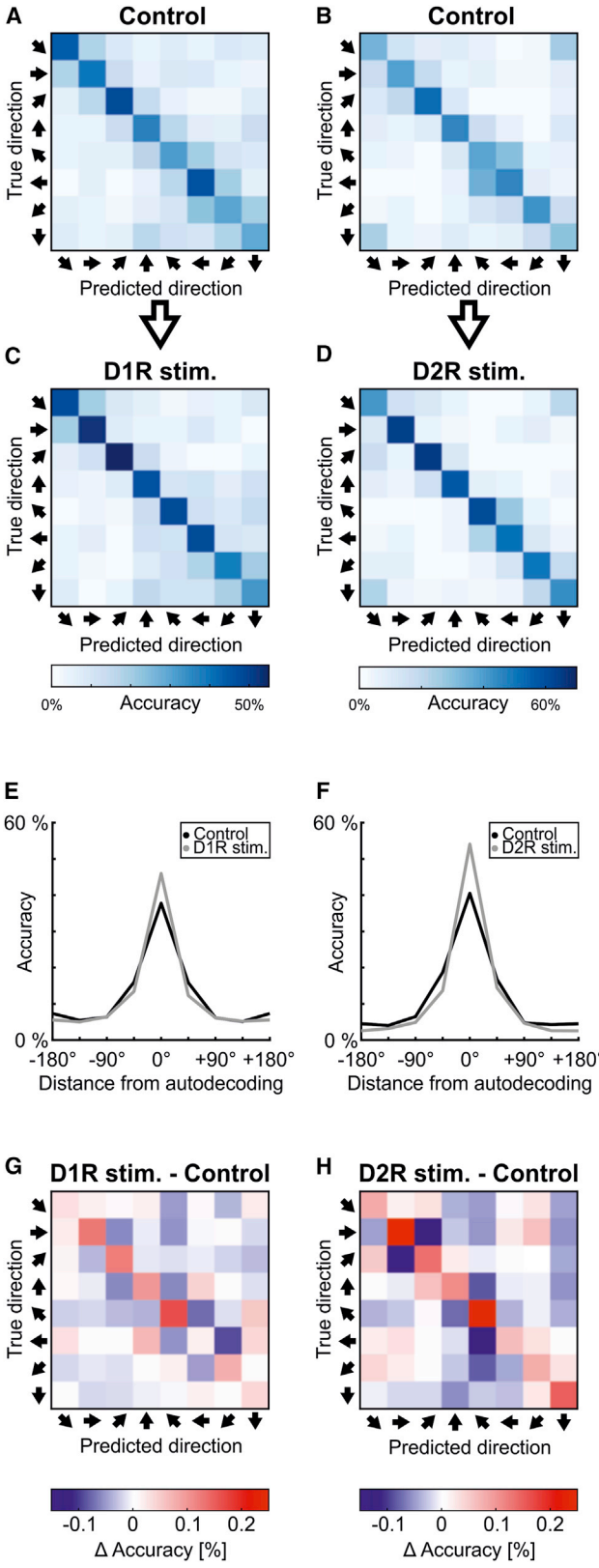


**Figure 5. Population Decoding Using SVM Classification**

(A and B) Confusion matrices show the performance accuracy of the classifiers in the control conditions (no drugs) on the basis of the two populations of neurons that were later tested with D1R or D2R stimulation (n = 37 and n = 45, respectively). The diagonal gives the performance of the classifier correctly decoding the eight directions.

(C and D) Same conventions as in (A) and (B), but now the classifiers are trained and tested with discharge rates elicited during dopamine receptor stimulation.

(E and F) Decoder tuning curves. Application of either the D1R or the D2R agonist increases the decoding performance.

(G and H) Confusion matrices showing the difference between the confusion matrices during control and dopamine receptor stimulation. Stimulation with either the D1R or the D2R agonist increased performance along the main diagonal and decreased misclassification on adjacent directions.

dopamine had positive coding effects on all selective neurons, irrespective of the quality of selectivity of individual neurons.

To allow a direct comparison of decoding performance between control and drug conditions, we calculated a difference confusion matrix (control − drug). For stimulation with both the D1R agonist (Figure 5G) and the D2R agonist (Figure 5H), decoding performance increases along the main diagonal with stimulation (see also Figures 5E and 5F at distance 0° from autodecoding). At the same time, the difference confusion matrix illustrates less confusion of the classifier in the drug conditions with the directly adjacent directions, as indicated by the blue squares (Figures 5G and 5H). The amount of information about motion directions represented by the populations of direction-selective neurons increased with stimulation of the D1 and D2 receptors. In agreement with the gating hypothesis, dopamine receptor stimulation renders PFC networks more ready to represent sensory input.

## DISCUSSION

In agreement with the overall hypothesis that dopamine in PFC provides a gating signal to enable privileged access of sensory information to PFC circuits (Braver and Cohen, 1999; Cohen et al., 2002; Ott and Nieder, 2019), we found that pharmacological stimulation of dopamine receptors enhanced the sensory sensitivity of PFC neurons tuned to visual motion direction. Stimulation of both D1Rs and D2Rs resulted in an increase of the signal-to-noise ratio (as measured by the auROC) of the neurons' responses. This sensitivity enhancement was particularly prominent for D2R stimulation (with quinpirole) and less pronounced for D1R stimulation (using SKF81297).

Although we did not directly test the effects of positive ejection currents in the present study, our previous iontophoretic experiments using exactly the same apparatus and methods ensure that the neuronal effects were not caused by current injection. We had previously shown in a total of four studies and identical techniques from our lab that dopaminergic effects in monkey PFC were not the result of nonspecific electrical current injection (Jacob et al., 2013; Ott and Nieder, 2017; Ott et al., 2014, 2018). In none of these studies did we observe that control injections of 0.9% physiological NaCl with ejection current between +25 and +50 nA had any impact on neuronal responses or neuronal coding capabilities in any sensory or delay trial phase. For instance, the representation of sensory signals in PFC was

unaltered by saline current injections; in addition, modulatory drug effects were specific for cells sensitive to dopamine (Jacob et al., 2013). This indicates that the dopaminergic neuronal effects were not the result of nonspecific electrical currents. A corresponding absence of potential current effects on single neurons was reported for monkeys engaged in a complex rule-switching task that consisted of a series of trial phases, such as fixation, sample presentation, working memory, rule cue, and choice delay periods; in all of these phases, the neuronal discharges and coding capacities were entirely unaffected by ejection currents applied to physiological NaCl (Ott et al., 2014, 2018). Finally, when we recorded local field potentials (LFPs) from the primate PFC while applying substances using microiontophoresis, the frequency band-specific oscillations were completely unchanged during control experiments with physiological saline (Ott et al., 2018). Application of normal saline did not produce changes in LFP power during any of the trial phase within a complex rule-based choice task. In sum, current injection cannot explain our findings.

### Mechanisms of How Dopamine Provides a Gating Signal in PFC

Several lines of evidence point toward a mechanism by which dopamine provides a fast gating signal allowing sensory and contextual information to enter PFC circuits (Ott and Nieder, 2019). At the levels of both single neurons and populations of selective neurons, we demonstrate that dopamine receptor stimulation enhances coding quality, thus rendering PFC networks more prone to accept and represent sensory input. Recordings from primate midbrain dopamine neurons during stimulus detection revealed that these neurons were active only when the animals successfully detected a stimulus (de Lafuente and Romo, 2011). Notably, the latency of dopamine neurons that reflected the monkeys' choice matched the latency of neuronal choice signals in frontal cortex that were delayed relative to visual signals in sensory cortex (de Lafuente and Romo, 2012). Thus, dopamine transients in PFC seem to provide a gating signal that permits sensory input to become updated and later stored in working memory (Braver and Cohen, 1999; Cohen et al., 2002). Human functional imaging supports this hypothesis by finding activity of midbrain dopaminergic nuclei that predicted the responses of context-dependent signals in PFC as well as the behavioral performance of subjects required to make context-dependent decisions (D'Ardenne et al., 2012). This is again consistent with the timing of a gating signal that regulates the encoding of representations in PFC.

What might be the mechanism behind dopaminergic gating? The present data suggest that enhancement of neuronal sensitivity is the prime factor. Surprisingly, neither D1R nor D2R stimulation had any impact on the neurons' tuning sharpness. This argues that the dopaminergic gating signal does not act via filtering in the sensory parameter space but through changes of neuronal sensitivity or gain. Gain modulation is an important mechanism to increase the signal detection capability of single cortical neurons (Servan-Schreiber et al., 1990). Dopamine itself can increase the overall activity of distinct groups of PFC neurons by a gain computation (Jacob et al., 2013). In a previous study, dopamine also reduced the variability of neuronal responses (Jacob et al., 2013); however, we could not demonstrate such an effect at the level of specific receptor families. Collectively, the findings suggest that dopamine gates visual signals in PFC neurons by increasing their sensitivity.

### The Role of the D2R Family

Pharmacological stimulation with receptor-specific drugs allowed us to separately address the roles of the two major dopamine receptor families. D2R stimulation resulted in the most prominent increase in neuronal sensitivity (as measured by auROC). This enhancement in motion direction sensitivity was caused by stronger activation of the neurons to the preferred motion direction. This finding contrasts the sensitivity mechanisms described for rule-selective signals; after D2R stimulation, rule-coding neurons showed enhanced coding not via an increase in responses to the preferred rule but through a reduction of responses to the non-preferred rule (Ott et al., 2014). Reduced discharge rate variability, however, does not seem to be a mechanism for increased sensitivity. D2R stimulation did not reduce the discharge variability of motion tuned neurons as measured by the FF, for the response neither to the preferred nor to the least preferred direction. This finding is in agreement with effects described for rule-selective activity, which also did not change by D2R stimulation (Ott et al., 2014).

We did not find a change in tuning selectivity (i.e., the tuning width of the PFC neurons to motion directions) under D2R stimulation. Assuming that the absence of enhanced tuning selectivity was not the result of relatively coarse sampling of motion directions, we suggest that an increase in response gain is responsible for the observed coding enhancement. Gain computation mediated by D2Rs is proposed to enhance sensory coding by excitatory mechanisms (Ott and Nieder, 2019). We speculate that parvalbumin (PV)-expressing, soma-targeting interneurons, which express D2Rs particularly strongly, might play an important role in this kind of gain modulation (Wilson et al., 2012).

### The Role of the D1R Family

In contrast to the clear sensitivity effects after D2R stimulation, D1R stimulation resulted in a more subtle enhancement. Still, we found an overall increase of coding sensitivity after D1R stimulation, both in the classifier population decoding approach and for single neurons when preferred and non-preferred responses were evaluated in the auROC analysis. The current effects for a basic visual parameter (motion direction) agree with our previous finding that D1R stimulation increased coding strength (as measured by auROCs) of PFC neurons to the presentation of abstract quantities. However, this increased coding of numerical quantity appeared on the background of an overall weak response inhibition by D1R stimulation (Jacob et al., 2016; Ott et al., 2014), an effect we did not replicate in the present study. A weak inhibition would speak against a gain modulation by D1Rs but favor a subtracting computation of shunting inhibition (Jacob et al., 2013; Ott and Nieder, 2019).

The precise mechanism behind this enhanced sensitivity after D1R stimulation was difficult to extract. This is because neither the tendency to modulate the response to the preferred and least preferred directions nor the tentative reduction in discharge rate

variability alone can explain the overall coding betterment. It seems that a combination of all of these effects, even though not significant on their own with a relatively small sample size, provide the most parsimonious explanation for the observed enhancement of response sensitivity.

*In vitro* studies have suggested that the enhancement of neuronal sensitivity is related to inhibitory mechanisms. D1Rs are known to decrease glutamate-induced excitatory post-synaptic currents (Gao et al., 2001; Seamans et al., 2001; Urban et al., 2002). This potentially decreases the output firing of these neurons by a constant amount ("subtraction computation"), which in turn could enhance the strength of signals arriving in PFC compared with background activity. As a potential cell class involved in this process, somatostatin-expressing dendrite-targeting interneurons are known to mediate subtractive shifts of neuronal responses in visual cortex (Wilson et al., 2012). However, our data do not support such an inhibitory mechanism. None of the many discharge parameters we analyzed indicated inhibition as a cause for sensory sensitivity.

## Conclusion

Together, these data help explain how dopamine exerts receptor-specific effects on PFC neurons that encode sensory stimuli. The representation of the direction of visual stimuli was significantly enhanced during dopamine receptor stimulation, albeit for the two receptor families to different degrees and on the basis of different mechanisms. These mechanisms show how dopaminergic input enables gating of relevant information when processing sensory input entering the PFC as the highest cognitive brain center. Although gating by D1Rs seems to rely on the summed impact of a variety of subtle mechanisms, D2R stimulation has clear and prominent effects on the neurons' coding quality. These effects are expected to be inverted after application of D1R and D2R antagonists in future studies.

## STAR★METHODS

Detailed methods are provided in the online version of this paper and include the following:

- KEY RESOURCES TABLE
- LEAD CONTACT AND MATERIALS AVAILABILITY
- EXPERIMENTAL MODEL AND SUBJECT DETAILS
- METHOD DETAILS
  - Experimental setup
  - Behavioral protocol
  - Surgery
  - Recording and drug application
- QUANTIFICATION AND STATISTICAL ANALYSIS
  - Direction-selective neurons
  - Single-cell and population responses
  - Tuning curve fit
  - Tuning width analysis
  - Receiver operating characteristic analysis
  - Fano factor
- DATA AND CODE AVAILABILITY

## ACKNOWLEDGMENTS

We thank Torben Ott for comments on this manuscript. This research was supported by DFG FOR 1847 grants NI 618/5-1 and NI 618/5-2 to A.N.

## AUTHOR CONTRIBUTIONS

M.S. and A.N. designed the experiment. M.S. recorded the data. M.S. and S.W. analyzed the data. M.S. and A.N. wrote the paper. A.N. supervised the study.

## DECLARATION OF INTERESTS

The authors declare no competing interests.

Received: August 26, 2019
Revised: October 22, 2019
Accepted: November 20, 2019
Published: December 24, 2019

## REFERENCES

Asaad, W.F., Rainer, G., and Miller, E.K. (2000). Task-specific neural activity in the primate prefrontal cortex. J. Neurophysiol. *84*, 451–459.

Björklund, A., and Dunnett, S.B. (2007). Dopamine neuron systems in the brain: an update. Trends Neurosci. *30*, 194–202.

Braver, T.S., and Cohen, J.D. (1999). Dopamine, cognitive control, and schizophrenia: the gating model. Prog. Brain Res. *121*, 327–349.

Chang, C., and Lin, C. (2011). LIBSVM. ACM Trans. Intell. Syst. Technol. *2*, 1–27.

Cohen, M.R., and Maunsell, J.H.R. (2009). Attention improves performance primarily by reducing interneuronal correlations. Nat. Neurosci. *12*, 1594–1600.

Cohen, J.D., Braver, T.S., and Brown, J.W. (2002). Computational perspectives on dopamine function in prefrontal cortex. Curr. Opin. Neurobiol. *12*, 223–229.

Constantinidis, C., Franowicz, M.N., and Goldman-Rakic, P.S. (2001). The sensory nature of mnemonic representation in the primate prefrontal cortex. Nat. Neurosci. *4*, 311–316.

D'Ardenne, K., Eshel, N., Luka, J., Lenartowicz, A., Nystrom, L.E., and Cohen, J.D. (2012). Role of prefrontal cortex and the midbrain dopamine system in working memory updating. Proc. Natl. Acad. Sci. U S A *109*, 19900–19909.

de Lafuente, V., and Romo, R. (2011). Dopamine neurons code subjective sensory experience and uncertainty of perceptual decisions. Proc. Natl. Acad. Sci. U S A *108*, 19767–19771.

de Lafuente, V., and Romo, R. (2012). Dopaminergic activity coincides with stimulus detection by the frontal lobe. Neuroscience *218*, 181–184.

Eiselt, A.-K., and Nieder, A. (2013). Representation of abstract quantitative rules applied to spatial and numerical magnitudes in primate prefrontal cortex. J. Neurosci. *33*, 7526–7534.

Eshel, N., Bukwich, M., Rao, V., Hemmelder, V., Tian, J., and Uchida, N. (2015). Arithmetic and local circuitry underlying dopamine prediction errors. Nature *525*, 243–246.

Everling, S., Tinsley, C.J., Gaffan, D., and Duncan, J. (2002). Filtering of neural signals by focused attention in the monkey prefrontal cortex. Nat. Neurosci. *5*, 671–676.

Freedman, D.J., Riesenhuber, M., Poggio, T., and Miller, E.K. (2001). Categorical representation of visual stimuli in the primate prefrontal cortex. Science *291*, 312–316.

Funahashi, S., Bruce, C.J., and Goldman-Rakic, P.S. (1989). Mnemonic coding of visual space in the monkey's dorsolateral prefrontal cortex. J. Neurophysiol. *61*, 331–349.

Gao, W.-J., Krimer, L.S., and Goldman-Rakic, P.S. (2001). Presynaptic regulation of recurrent excitation by D1 receptors in prefrontal circuits. Proc. Natl. Acad. Sci. U S A *98*, 295–300.

Hussar, C.R., and Pasternak, T. (2009). Flexibility of sensory representations in prefrontal cortex depends on cell type. Neuron *64*, 730–743.

Hussar, C.R., and Pasternak, T. (2013). Common rules guide comparisons of speed and direction of motion in the dorsolateral prefrontal cortex. J. Neurosci. *33*, 972–986.

Jacob, S.N., and Nieder, A. (2014). Complementary roles for primate frontal and parietal cortex in guarding working memory from distractor stimuli. Neuron *83*, 226–237.

Jacob, S.N., Ott, T., and Nieder, A. (2013). Dopamine regulates two classes of primate prefrontal neurons that represent sensory signals. J. Neurosci. *33*, 13724–13734.

Jacob, S.N., Stalter, M., and Nieder, A. (2016). Cell-type-specific modulation of targets and distractors by dopamine D1 receptors in primate prefrontal cortex. Nat. Commun. *7*, 13218.

Kim, J.-N., and Shadlen, M.N. (1999). Neural correlates of a decision in the dorsolateral prefrontal cortex of the macaque. Nat. Neurosci. *2*, 176–185.

Merten, K., and Nieder, A. (2012). Active encoding of decisions about stimulus absence in primate prefrontal cortex neurons. Proc. Natl. Acad. Sci. U S A *109*, 6289–6294.

Miller, E.K., and Cohen, J.D. (2001). An integrative theory of prefrontal cortex function. Annu. Rev. Neurosci. *24*, 167–202.

Nieder, A., Freedman, D.J., and Miller, E.K. (2002). Representation of the quantity of visual items in the primate prefrontal cortex. Science *297*, 1708–1711.

Ott, T., and Nieder, A. (2017). Dopamine D2 receptors enhance population dynamics in primate prefrontal working memory circuits. Cereb. Cortex *27*, 4423–4435.

Ott, T., and Nieder, A. (2019). Dopamine and cognitive control in prefrontal cortex. Trends Cogn. Sci. *23*, 213–234.

Ott, T., Jacob, S.N., and Nieder, A. (2014). Dopamine receptors differentially enhance rule coding in primate prefrontal cortex neurons. Neuron *84*, 1317–1328.

Ott, T., Westendorff, S., and Nieder, A. (2018). Dopamine receptors influence internally generated oscillations during rule processing in primate prefrontal cortex. J. Cogn. Neurosci. *30*, 770–784.

Rainer, G., Asaad, W.F., and Miller, E.K. (1998a). Memory fields of neurons in the primate prefrontal cortex. Proc. Natl. Acad. Sci. U S A *95*, 15008–15013.

Rainer, G., Asaad, W.F., and Miller, E.K. (1998b). Selective representation of relevant information by neurons in the primate prefrontal cortex. Nature *393*, 577–579.

Redgrave, P., and Gurney, K. (2006). The short-latency dopamine signal: a role in discovering novel actions? Nat. Rev. Neurosci. *7*, 967–975.

Schultz, W. (2016). Dopamine reward prediction-error signalling: a two-component response. Nat. Rev. Neurosci. *17*, 183–195.

Schultz, W., Dayan, P., and Montague, P.R. (1997). A neural substrate of prediction and reward. Science *275*, 1593–1599.

Seamans, J.K., and Yang, C.R. (2004). The principal features and mechanisms of dopamine modulation in the prefrontal cortex. Prog. Neurobiol. *74*, 1–58.

Seamans, J.K., Gorelova, N., Durstewitz, D., and Yang, C.R. (2001). Bidirectional dopamine modulation of GABAergic inhibition in prefrontal cortical pyramidal neurons. J. Neurosci. *21*, 3628–3638.

Servan-Schreiber, D., Printz, H., and Cohen, J. (1990). A network model of catecholamine effects: gain, signal-to-noise ratio, and behavior. Science *249*, 892–895.

Stauffer, W.R., Lak, A., Yang, A., Borel, M., Paulsen, O., Boyden, E.S., and Schultz, W. (2016). Dopamine neuron-specific optogenetic stimulation in rhesus macaques. Cell *166*, 1564–1571.e6.

Steinberg, E.E., Keiflin, R., Boivin, J.R., Witten, I.B., Deisseroth, K., and Janak, P.H. (2013). A causal link between prediction errors, dopamine neurons and learning. Nat. Neurosci. *16*, 966–973.

Thiele, A., Delicato, L.S., Roberts, M.J., and Gieselmann, M.A. (2006). A novel electrode-pipette design for simultaneous recording of extracellular spikes and iontophoretic drug application in awake behaving monkeys. J. Neurosci. Methods *158*, 207–211.

Urban, N.N., González-Burgos, G., Henze, D.A., Lewis, D.A., and Barrionuevo, G. (2002). Selective reduction by dopamine of excitatory synaptic inputs to pyramidal neurons in primate prefrontal cortex. J. Physiol. *539*, 707–712.

Vallentin, D., Bongard, S., and Nieder, A. (2012). Numerical rule coding in the prefrontal, premotor, and posterior parietal cortices of macaques. J. Neurosci. *32*, 6621–6630.

Wallis, J.D., Anderson, K.C., and Miller, E.K. (2001). Single neurons in prefrontal cortex encode abstract rules. Nature *411*, 953–956.

Williams, S.M., and Goldman-Rakic, P.S. (1998). Widespread origin of the primate mesofrontal dopamine system. Cereb. Cortex *8*, 321–345.

Wilson, N.R., Runyan, C.A., Wang, F.L., and Sur, M. (2012). Division and subtraction by distinct cortical inhibitory networks in vivo. Nature *488*, 343–348.

Zaksas, D., and Pasternak, T. (2006). Directional signals in the prefrontal cortex and in area MT during a working memory for visual motion task. J. Neurosci. *26*, 11726–11742.

# STAR★METHODS

## KEY RESOURCES TABLE

| REAGENT or RESOURCE | SOURCE | IDENTIFIER |
|---|---|---|
| Chemicals, Peptides, and Recombinant Proteins | | |
| SKF81297 | Sigma aldrich | S179 ; CAS ID 253446-15-0 |
| quinpirole | Sigma aldrich | Q102; CAS ID 85798-08-9 |
| Experimental Models: Organisms/Strains | | |
| Macaca mulatta | German Primate Centre, Göttingen | https://www.dpz.eu |
| Software and Algorithms | | |
| NIMH Cortex | National Institute of Mental Health | c598; https://www.nimh.nih.gov/research/research-conducted-at-nimh/research-areas/clinics-and-labs/ln/shn/software-projects.shtml |
| MAP Data Acquisition System | Plexon | https://plexon.com/ |
| MATLAB R2018a | MathWorks | https://www.mathworks.com |
| LIBSVM version 3.23 | Chang and Lin, 2011 | https://www.csie.ntu.edu.tw/~cjlin/libsvm/ |
| Other | | |
| Dental Cement | Heraeus | Paladur, ISO 20795, CE 0197 |
| Microdrives | Modified NAN C-drive | http://naninstruments.com/ |
| Electrodes | Animal Physiology Unit | Custom fabrication |

## LEAD CONTACT AND MATERIALS AVAILABILITY

Further information and requests for resources and reagents should be directed to and will be fulfilled by the Lead Contact, Andreas Nieder (andreas.nieder@uni-tuebingen.de).

This study did not generate new unique reagents.

## EXPERIMENTAL MODEL AND SUBJECT DETAILS

We used two 8-year-old, healthy male rhesus monkeys (Macaca mulatta) (monkey X and monkey D, respectively) that were obtained from the German Primate Centre (DPZ) in Göttingen and indoor housed in social groups. The monkeys were on a controlled feeding protocol during the training and recording period and their body weight was measured daily during that time. The daily amount of water was given as reward during, or if necessary after the sessions. Food was available *ad libitum* in the group cage. All experimental procedures were in accordance with the guidelines for animal experimentation determined by the responsible authority, the Regierungspräsidium Tübingen.

## METHOD DETAILS

### Experimental setup

The experiment was conducted in a darkened operant conditioning chamber. The monkeys were seated in a primate chair in front of a computer screen that was used for the display of the visual stimuli. The animals used a metal bar to indicate their behavioral choices. Fluid reward was delivered by an automated reward system via a mouthpiece that was attached to the chair. CORTEX software (NIMH, Bethesda, MD) was used for experimental control and behavioral data acquisition. During each trial the monkey had to maintain eye fixation within 3.5° visual angle of the central fixation target (ISCAN). Neuronal data was recorded using a PLEXON system (Plexon Inc., Dallas, Texas).

### Behavioral protocol

The monkeys were trained to watch a series of visual random dot patterns moving in the center of the screen. Stimuli were circular patches of random dots 5° of visual angle (dva) in diameter. The overall dot density was 12 per dva$^2$ with a radius of 0.04 dva for each dot and they moved with 100% coherence at a speed of 4 dva/s. The movement of the dots varied in eight directions, spaced evenly across the full 360°. The color of all dots was a light gray. All stimuli were generated using MATLAB (The MathWorks).

A trial was initiated by holding a metal bar and maintaining gaze on a central fixation target (fixation period). After 300 ms, a series of eight stimuli of pseudo-randomized motion directions was presented in sequence. At the end of each trial, a fluid reward was delivered if the monkey maintained holding the bar and maintained fixation throughout the stimulus presentation sequence. Each

stimulus was presented for 300 ms and contained dot patterns moving in one of eight directions. Within one trial every possible direction was presented only once and the time between each stimulus was 100 ms. This passive fixation task in which the monkey only observed moving dot patterns (data of the current paper) was interleaved with trial blocks in which the monkey was actively engaged in a delayed response task (not reported here).

### Surgery

The surgery was performed while the monkeys were under general anesthesia. The animals were placed in a stereotaxic holder and implanted with titanium headposts and a recording chamber over the lateral PFC in the right hemisphere. The chamber was placed centrally over the posterior part of the principal sulcus, anterior to the sulcus arcuatus in both animals guided by landmarks obtained through MRI and stereotactic measurements, acquired prior to the surgeries. Recordings were performed equally in all available cortex without bias.

### Recording and drug application

Extracellular recordings and micro-iontophoretic drug application were performed as described previously (Jacob et al., 2013, 2016; Ott et al., 2014). On each session, up to three custom-made, tungsten-in-glass electrodes (Thiele et al., 2006) with two flanking barrels were lowered transdurally into the brain using a modified electrical drive (NAN Drive). We randomly recorded single neurons and made no attempt to preselect task-selective neurons. Signal acquisition, filtering, amplification and digitalization were accomplished with the MAP system (Plexon). Waveform separation was performed offline (Offline Sorter; Plexon).

Electrode impedances were measured after the recordings and ranged between 0.5 and 3.5 MΩ (measured at 500 Hz; Omega Tip Z; World Precision Instruments). The pipette impedances typically ranged between 15-50 MΩ (full range: 10-350 MΩ) and were dependent on the opening diameter. As described previously (Jacob et al., 2013, 2016; Ott et al., 2014) we used retention currents for all drugs of −7 nA. The D1 receptor (D1R) agonist SKF81297 (Sigma-Aldrich) was applied using ejection currents of +15 nA. For the D2 receptor (D2R) agonist quinpirole (Sigma-Aldrich) ejection currents of +40 nA were used. Both drugs were dissolved in ultra-pure, double distilled water at a concentration of 10 mM and a pH of 4.0 using HCl. For every recording day either SKF81297 or quinpirole was chosen and filled into one barrel per electrode. The other barrel was always filled with 0.9% NaCl to prevent excess drug solution to spill over into this barrel during the filling process. During the recording, iontophoresis conditions without (control) and with drug application (drug) alternated in blocks. Only one drug was tested per recording session.

Each recording day started with a control block followed by a drug block. On average, the length of control and drug blocks was 15 min, depending on the time the monkeys spent to do 108 correct trials. Retention (control phase) or ejection (drug phase) periods lasted for the full duration of a block, i.e., about 15 min. As iontophoretic drug application is fast and has been shown to modulate neuronal discharge rates quickly (Jacob et al., 2013; Ott et al., 2014), no data was excluded at the current switching points. Once the first drug block was finished, another control block followed by another drug block commenced. This sequence was repeated up to three times (i.e., three control and three drug blocks) until the monkeys were saturated and stopped working. Data from up to six successive blocks (or up to three control-drug successions, respectively) were analyzed, thus preventing systematic distortions of dopaminergic effects based on potential drifts of physiological conditions over time.

In previous iontophoretic experiments using exactly the same apparatus and methods, we have ensured that neuronal effects are not caused by positive ejection currents (Jacob et al., 2013; Ott et al., 2014). In such control experiments with 0.9% physiological NaCl and ejection currents of up to +40 nA (as used here), none of the tested neuronal responses, neither spontaneous activity nor any of the selective responses, were affected by ejection currents alone (Jacob et al., 2013; Ott et al., 2014).

## QUANTIFICATION AND STATISTICAL ANALYSIS

All data analysis was performed using the R2018a release of MATLAB software. For neuronal population analysis, the data from both monkeys were pooled as they showed similar results. We used the same time window for all analysis and drugs as described in section 'Direction-selective neurons'.

The following statistical tests were used as appropriate for the data: two factorial analysis of variance to define direction selective neurons. A chi-square test to test the frequency of direction selective neurons between monkeys. A Rayleigh test for circular uniformity of preferred directions of direction selective neurons. A Wilcoxon rank sum test to test for effects of drug application to the preferred or least-preferred direction on a single cell level. A paired Wilcoxon test for the same as the previous analysis on the level of the population of direction selective neurons. The paired Wilcoxon test was further used to test for the effects of drug application on the direction sensitivity (auROC), the Fano factor and differences in the goodness of fit on a population level. Changes in tuning width, as measured by Gaussian fit and full-width at half-height, were also tested using a paired Wilcoxon test. The influence of drug application on the decoding performance (SVM) was tested using a random permutation test.

Data were presented as mean ± standard error of the mean (SEM) unless indicated otherwise. $p < 0.05$ was considered to be statistically significant.

For all analyses the exact statistical test including the p values, dispersion and precision measures are given in the results section.

### Direction-selective neurons

All neurons recorded with at least 10 correct trials per motion direction in both the control and drug conditions were included in the analysis. A two factorial analysis of variance (ANOVA) with direction (eight levels: 0° to 315°) and iontophoresis condition (levels: control and drug) was performed on the discharge rates during stimulus presentation (0.18 s to 0.48 s after stimulus onset) on the pool of 296 recorded neurons. Neurons were counted as direction selective if they were significant for the main factor direction ($p < 0.05$). None of the reported results depended on the exact choice of time window for the analysis. Similar results were obtained using different parameters. All further analyses were performed on the pool of direction selective neurons as determined by the ANOVA ($n = 82$).

### Single-cell and population responses

For single-cell responses, spike-density functions were generated, i.e., individual trials were parsed in 10 ms bins and spikes convoluted with a Gaussian function with a width of sigma = 25 ms. Activity was then averaged for every 10 ms bin over all trials of a given direction.

### Tuning curve fit

Each direction-selective neuron was fit with a Gaussian function to analyze the individual tuning curve. For the fitting we used the four parameters, maximum response (a), preferred direction (b), width (c) and offset (d); see Equation 1. MATLABs 'nonlinearleastsquares' algorithm was used to find optimal values for each neuron. For the example neurons in Figure 2, raw discharge rates were used to compute the tuning curves. For the population tuning curves, we used baseline-corrected discharge rates to account for the influence of the drug on the neurons' baseline level. To that aim, from all responses to the different directions in control and drug condition we subtracted the average baseline response separately for drug and control condition (e.g., responses in control minus average baseline in control). For each direction we calculated the error across trials as standard error of the mean (SEM).

To generate population tuning curves, all responses were aligned to the preferred direction and averaged over all neurons for each iontophoresis condition separately. The average response was then used to fit the population tuning curve using the same fitting procedure as for the example neurons. For each direction we calculated the error across neurons as standard error of the mean (SEM).

$$f(x) = a * e^{-\left(\frac{x-b}{c}\right)^2} + d \qquad \text{Equation 1}$$

### Tuning width analysis

A second measure to describe the tuning width was the full-width at half-height of each neurons raw direction tuning profile. Like for the Gaussian fits, we used the baseline-corrected discharge rates to account for changes in the baseline level induced by the drug application. For all neurons we calculated the width of the tuning profile at 50% of their maximum response for control- and drug condition separately.

#### *Multi-Class Support Vector (SVM) classification*

To assess the directional information contained in the population of direction-selective neurons and to evaluate how this information changes with dopamine receptor stimulation, we trained a multi-class SVM classifier (Chang and Lin, 2011) (LIBSVM version 3.23). We used a linear SVM-kernel with default parameter settings and applied 'one-versus-one' classification to distinguish our eight directions. A separate classifier was built for each iontophoresis condition using 20 trials per neuron. For neurons with more than 20 trials we randomly sampled without replacement 20 trials. A small subset of 15% of our direction-selective neurons (13/82) was recorded with 10 to 19 trials. For these neurons we added the missing number of trials by randomly sampling with replacement from the pool of their trials. Thus, the SVM training and test datasets were completely distinct for 85% of the neurons; for the remaining 15% of the neurons, the training and test datasets mildly overlapped. We normalized all discharge rates by z-scoring and used leave-one-out cross-validation. In the confusion matrix the main diagonal contains correct labeling of the classifier. By averaging over the main and minor diagonals of the confusion matrix we calculated the decoding tuning curve. This process was repeated 1000 times and in each run the difference in average decoding performance between drug application and control (performance drug – performance control) was calculated. The application of the dopamine receptor agonists was considered to significantly increase the decoding performance, if less of than 5% of the distribution of differences was negative.

### Receiver operating characteristic analysis

To quantify the direction tuning selectivity, we used the receiver operating characteristic (ROC), which is a measure derived from the signal detection theory. For each direction selective neuron ($n = 82$) the ROC curve was generated by calculating the true positive rate (discharge rate in response to the preferred direction) and the false positive rate (discharge rate in response to the least-preferred direction) in each iontophoresis condition. Using the direction 180° opposite of the preferred direction as false positive yielded similar results. We then calculated the area und the ROC curve (auROC). The auROC is a nonparametric measure of the discriminability of two distributions and denotes the probability, by which an ideal observer is able to differentiate a meaningful signal from a noisy

background. A perfect discrimination yields values of 1, while no separation is given by values of 0.5. As the auROC takes into account both the difference between distributions means and their width, it is a good indicator of signal quality.

### Fano factor

We calculated the Fano factor (FF) to quantify the impact of drug on the response variability. As the mean-normalized dispersion, we calculated the Fano factor (variance/mean) for each direction selective neuron (n = 82) by dividing the variance, $\sigma^2$, of the distribution of discharge rates by its mean, $\mu$. The FF was calculated for the preferred and least preferred direction in each iontophoresis condition separately.

## DATA AND CODE AVAILABILITY

The dataset and analysis-specific code have not been deposited in a public repository because the data await further analyses by the authors. The analysis-specific code is available from the corresponding author on request.